Demonstration of the role of cell wall homeostasis in *Staphylococcus aureus* growth and the action of bactericidal antibiotics

Bartłomiej Salamaga[a,b,1], Lingyuan Kong[c,1], Laia Pasquina-Lemonche[b,d,1], Lucia Lafage[a,b,1], Milena von und zur Muhlen[a,b,1], Josie F. Gibson[a,b,e], Danyil Grybchuk[f], Amy K. Tooke[a,b], Viralkumar Panchal[a,b], Elizabeth J. Culp[g], Elizabeth Tatham[a,b], Mary E. O'Kane[d], Thomas E. Catley[d], Stephen A. Renshaw[b,e,h], Gerard D. Wright[g], Pavel Plevka[f], Per A. Bullough[a], Aidong Han[c,2], Jamie K. Hobbs[b,d,2], and Simon J. Foster[a,b,2]

[a]School of Biosciences, University of Sheffield, Sheffield S102TN, United Kingdom; [b]The Florey Institute for Host-Pathogen Interactions, University of Sheffield, Sheffield S102TN, United Kingdom; [c]State Key Laboratory of Cellular Stress Biology, School of Life Sciences, Xiamen University, Xiamen 361102, China; [d]Department of Physics and Astronomy, University of Sheffield, Sheffield S37RH, United Kingdom; [e]The Bateson Centre, University of Sheffield, Sheffield S102TN, United Kingdom; [f]Central European Institute of Technology, Masaryk University, Brno 60177, Czech Republic; [g]M. G. DeGroote Institute for Infectious Disease Research, David Braley Centre for Antibiotic Discovery, Department of Biochemistry and Biomedical Sciences, McMaster University, Hamilton, ON L8S4L8, Canada; and [h]Department of Infection, Immunity and Cardiovascular Diseases, University of Sheffield, Sheffield S102RX, United Kingdom

Bacterial cell wall peptidoglycan is essential, maintaining both cellular integrity and morphology, in the face of internal turgor pressure. Peptidoglycan synthesis is important, as it is targeted by cell wall antibiotics, including methicillin and vancomycin. Here, we have used the major human pathogen *Staphylococcus aureus* to elucidate both the cell wall dynamic processes essential for growth (life) and the bactericidal effects of cell wall antibiotics (death) based on the principle of coordinated peptidoglycan synthesis and hydrolysis. The death of *S. aureus* due to depletion of the essential, two-component and positive regulatory system for peptidoglycan hydrolase activity (WalKR) is prevented by addition of otherwise bactericidal cell wall antibiotics, resulting in stasis. In contrast, cell wall antibiotics kill via the activity of peptidoglycan hydrolases in the absence of concomitant synthesis. Both methicillin and vancomycin treatment lead to the appearance of perforating holes throughout the cell wall due to peptidoglycan hydrolases. Methicillin alone also results in plasmolysis and misshapen septa with the involvement of the major peptidoglycan hydrolase Atl, a process that is inhibited by vancomycin. The bactericidal effect of vancomycin involves the peptidoglycan hydrolase SagB. In the presence of cell wall antibiotics, the inhibition of peptidoglycan hydrolase activity using the inhibitor complestatin results in reduced killing, while, conversely, the deregulation of hydrolase activity via loss of wall teichoic acids increases the death rate. For *S. aureus*, the independent regulation of cell wall synthesis and hydrolysis can lead to cell growth, death, or stasis, with implications for the development of new control regimes for this important pathogen.

peptidoglycan | antibiotics | cell wall | vancomycin | methicillin

How bacteria grow and divide is a fundamental question in microbiology, where many of the essential processes involved are the targets of clinically important antibiotics. The cell wall is crucial for bacterial survival, forming the interface between the external and internal environments and maintaining internal turgor pressure (1, 2). The major cell wall structural component is peptidoglycan (PG), a polymer of glycan strands and peptide cross-links (3–5), the synthesis of which is the target of antibiotics including β-lactams and glycopeptides (6). These cell wall antibiotics inhibit the final stages of PG synthesis where building blocks are incorporated into the existing structure via the action of penicillin-binding proteins (PBPs) (6). Several mechanisms linking the action of antibiotics to the inhibition of essential processes in cell wall growth and division have been suggested, including lytic and nonlytic death, oxidative stress, and futile PG synthesis (7–12).

As a single macromolecule that surrounds the cell, PG can increase in surface area to permit growth and division while maintaining cellular integrity. It has been proposed that areal PG growth occurs as a consequence of both synthesis and hydrolysis (4, 13, 14), with new material being covalently bound to the existing macrostructure and hydrolysis of existing bonds allowing expansion. This leads to a simple set of hypotheses for growth but also makes predictions as to the effects of inhibition of PG homeostasis activities, including cell wall antibiotics (Fig. 1A). The lack of either PG synthesis or hydrolysis will result in cell death because of the continued activity of the other, but the loss of both will lead to stasis.

Staphylococcus aureus is a major human antimicrobial-resistant pathogen. As a spheroid cell with a simple growth and division

Significance

The bacterial cell wall peptidoglycan is essential for maintenance of viability and yet is dynamic, permitting growth and division. Peptidoglycan synthesis is inhibited by important antibiotics, including β-lactams and vancomycin. Using the human pathogen *Staphylococcus aureus*, we have examined peptidoglycan homeostatic mechanisms and how their interruption leads to cell death. This has revealed two antibiotic-induced killing mechanisms mediated by specific peptidoglycan hydrolases, both involving the appearance of holes that span the entire thickness of the cell wall. One of the mechanisms is associated with growth and the other with cell division. This study supports a simple model for how cells grow via a combination of peptidoglycan synthesis and hydrolysis and how antibiotic intervention leads to cell death.
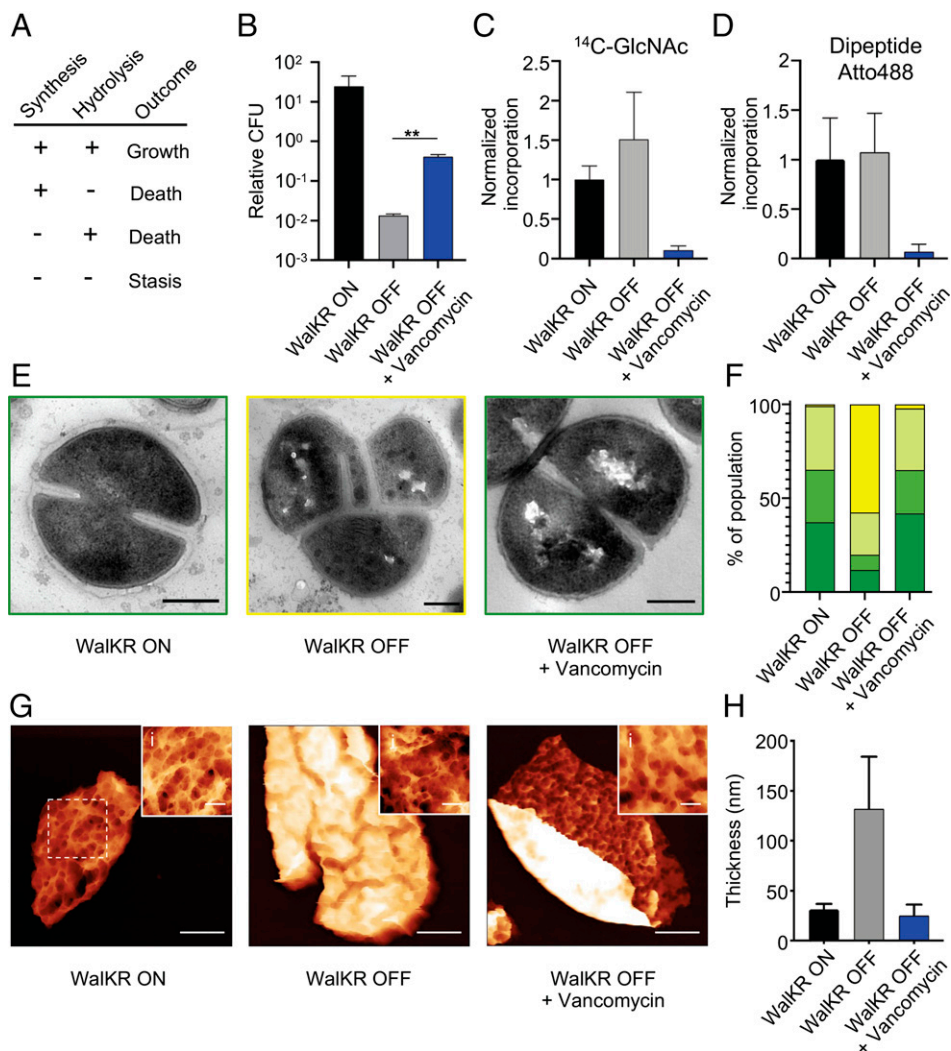
MICROBIOLOGY

Fig. 1. The role of regulation of PG hydrolases (PGHs) by WalKR in life and death. (*A*) Predictive model for how cell wall homeostasis governs bacterial life and death. Both cell wall synthesis and hydrolysis are required for growth, loss of either results in death, or both, cell stasis. (*B–H*) Effect of 10 × minimum inhibitory concentration (MIC) vancomycin for 3 h on conditional lethal strain *S. aureus* P$_{spac}$-*walKR* (without inducer; WalKR OFF) compared to the control (with inducer; WalKR ON). (*B*) CFU relative to T = 0; after *t* test with Welch's correction: *P* (WalKR OFF − WalKR OFF + vancomycin, **) = 6.9 × 10^{-3}. (*C* and *D*) PG synthesis and transpeptidase activity measured by ^{14}C-GlcNAc and Atto 488 dipeptide (53) incorporation, normalized against WalKR ON. (*E*) Transmission electron microscopy (TEM) (scale bars, 300 nm). (*F*) Quantification of bacterial phenotypes (*SI Appendix*, Fig. S2; dark green: no septum, mid-green: incomplete septum, light green: complete septum, and yellow: growth defects). For samples shown, the number of individual cells quantified was n > 300. (*G*) AFM topographic images of sacculi (scale bars, 150, 300, and 300 nm; data scales [DS], 85, 200, and 85 nm, respectively, from *Left* to *Right*). (*i*) Insets show sacculus external architecture from *Left* to *Right*, (WalKR ON) from dashed box in panel *G*, (WalKR OFF) from *SI Appendix*, Fig. S2E, (WalKR OFF+Van) from *SI Appendix*, Fig. S2D, respectively (scale bars, 50 nm; DS, 30, 52, and 32 nm, respectively, from *Left* to *Right*; images were analyzed with NanoscopeAnalysis from Bruker using the default color scale). (*H*) Thickness distribution values for sacculi with SD (n = 5). For sample size and data reproducibility, see *Materials and Methods*.

cycle, it forms an excellent subject to demonstrate the basic principles underlying growth, division, and the action of antibiotics. Many organisms have multiple PBPs, but *S. aureus* has only four, of which PBP1 and PBP2 are essential for growth and division (15–19). *S. aureus* also has many PG hydrolases (PGHs), including SagB, which is involved in cell growth (20, 21). The bifunctional Atl is involved in generalized cell lysis and cell separation after septation and contains both amidase and glucosaminidase domains (22, 23). PGHs often show functional redundancy with several enzymes involved in the same process (20, 24). In *S. aureus*, no individual PGH alone has been shown to be required for either growth or division, but multiple PGHs are positively regulated by an essential two-component system, WalKR (25–27), further suggesting that their collective activity is required.

Recently, using atomic force microscopy (AFM), we have revealed that the molecular architecture of the PG is that of an

expanded hydrogel whose mature external surface is a porous open network but with an interior surface characterized by a much smoother and denser mesh of PG material (28). This provides an architectural framework from which to begin to elucidate the roles of PG synthesis and hydrolysis. Here, we have taken an integrated approach to determine the role of PG homeostasis in *S. aureus* growth, division, and the bactericidal action of cell wall antibiotics.

Results

Role of PGHs in Growth and the Action of Antibiotics. *S. aureus* has many putative PGHs, mostly of unknown function (20, 24, 29, 30), many of which are positively regulated by an essential two-component system, WalKR (25–27). The loss of WalKR results in growth inhibition and cell morphology defects and

absence of lysis in the presence of penicillin (26, 31). We first verified the essentiality of WalKR using a conditional *S. aureus* strain (P*spac*-*walKR*) (32), where depletion of WalKR via removal of the inducer isopropyl β-D-thiogalactopyranoside (IPTG) led to >95% cell death within 3 h (Fig. 1*B* and *SI Appendix*, Fig. S1 *A* and *B*). Using the P*spac*-*walKR* strain and growth in the presence, or absence, of IPTG for 3 h, the role of WalKR was determined in cell wall dynamics (Fig. 1). We observed that death is concomitant with continued PG synthesis as measured by continued transglycosylase (¹⁴C-GlcNAc incorporation; Fig. 1*C*) and transpeptidase (Atto488 dipeptide incorporation; Fig. 1*D*) activities. Electron microscopy (EM) and AFM revealed this is associated with a thickening of the cell wall and aberrant septum formation (Fig. 1 *E–H* and *SI Appendix*, Fig. S2). We have recently shown that *S. aureus* PG has surface pores that do not penetrate the full thickness of the PG (28). The depletion of WalKR led to the maintenance of the pores, but they spanned a smaller fraction of the cell wall thickness (*SI Appendix*, Fig. S2 *H–M*). These data support the model whereby lack of processing by PGH leads to aberrant cell walls that do not permit growth and division, potentially contributing to cell death (Fig. 1*A*). We next tested whether prevention of PG synthesis in the absence of PGH activity would lead to stasis and rescue bacterial viability, as suggested by the model (Fig. 1*A*). Cell wall antibiotics, such as methicillin (a β-lactam) and vancomycin (a glycopeptide), are well-established inhibitors of PG synthesis. Vancomycin addition for 3 h led to stasis of the *walKR*-depleted cells, with significant reduction in cell death (Fig. 1*B*; $P = 6.9 \times 10^{-3}$), coincident with the inhibition of PG synthesis and lack of cell wall thickening (Fig. 1 *C–H* and *SI Appendix*, Fig. S2), as predicted (Fig. 1*A*). A significant reduction in cell death in *walKR*-depleted cells also occurred with the addition of methicillin (*SI Appendix*, Fig. S1*D*; $P = 6.3 \times 10^{-3}$), although this is only apparent at 3 h after antibiotic addition. That is, when both PG synthesis and hydrolysis are inhibited, bacterial cell death is

avoided (stasis). Previously, it has been shown that the constitutive expression of several PGH can complement the growth defect due to loss of WalKR, including ScaD (SsaA) (26). The *scaD* gene was chosen as it is regulated by WalKR (26) and *sagB*, as this is a major PGH (20) that has not been shown to be WalKR transcriptionally controlled. Notably, although constitutive expression of either PGH could complement the growth defect due to loss of WalKR, neither reversed the cell wall antibiotic stasis phenomenon, suggesting that multiple enzymes act collectively in antibiotic-associated cell death (*SI Appendix*, Fig. S1 *E–H*).

Effect of Cell Wall Antibiotics on Cellular Morphology. The simple model for growth (Fig. 1*A*) predicts that bactericidal antibiotics kill because of the inhibition of PG synthesis only when growth-associated PGH activity is present. To explore the cellular and molecular mechanisms involved, we characterized the impact of cell wall synthesis inhibiting antibiotics on morphology.

Treatment with vancomycin, methicillin, or a combination of both antibiotics led to 93 ± 5, 97 ± 2, and 92 ± 4% death after 6 h, respectively (Fig. 2*A*). Both antibiotics led to a significant increase in cell volume after 60 min treatment (Fig. 2*B*; $P = 5.835 \times 10^{-36}$ [methicillin] and $P = 3.262 \times 10^{-38}$ [vancomycin]), and this was not due to PG synthesis as, within 15 min, the incorporation of D-amino acids into PG was reduced to basal levels for both treatments (Fig. 2*C*). A similar inhibition of *N*-acetyl glucosamine incorporation into insoluble material was found for vancomycin, while residual incorporation was found for methicillin (Fig. 2*D*). The addition of methicillin led to swollen "bulbous" septa with apparent plasmolysis, where the membrane retracted away from the cell wall (Fig. 2 *E* and *F* and *SI Appendix*, Fig. S3*A*). These bulbous septa have been observed previously and have been associated with the killing mechanism of β-lactams (8). Conversely, vancomycin or a combination of both antibiotics did not lead to major morphological
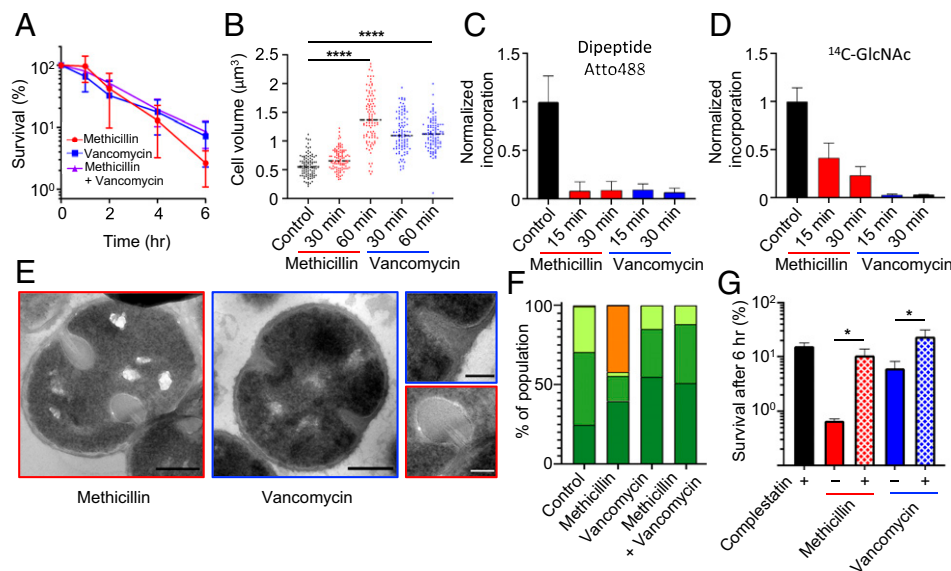
Fig. 2. The bactericidal action of cell wall antibiotics. Effect of 10 × MIC methicillin and/or vancomycin on *S. aureus* SH1000. (*A*) Survival of bacterial cells after addition of antibiotic(s). (*B*) Cell volume as measured by structured illumination microscopy (SIM) after N-hydroxysuccinimide(NHS)-ester AlexaFluor 405 labeling. After *t* test with Welch's correction: P (control − methicillin 60 min, ****) = 5.835×10^{-36}, P (control − vancomycin 60 min, ****) = 3.262×10^{-38}. For each sample, $n > 100$. (*C* and *D*) PG synthesis and transpeptidase activity measured by Atto 488 dipeptide and ¹⁴C-GlcNAc incorporation. (*E*) TEM. (scale bars, 300 nm). (*F*) Quantification of bacterial phenotypes (*SI Appendix*, Fig. S3; dark green: no septum, mid-green: incomplete septum, light green: complete septum, and orange: plasmolysis). For samples shown, the number of individual cells quantified was $n > 300$. (*G*) Effect of 5 × MIC complestatin on *S. aureus* SH1000 survival rate after 6 h, treated with methicillin or vancomycin. CFU relative to T = 0. After *t* test with Welch's correction: P (methicillin − methicillin + complestatin, *) = 3.45×10^{-2}, P (vancomycin − vancomycin + complestatin, *) = 4.01×10^{-2}. For sample size and data reproducibility, see *Materials and Methods*.

Salamaga et al.
Demonstration of the role of cell wall homeostasis in *Staphylococcus aureus* growth and the action of bactericidal antibiotics

PNAS | 3 of 8
https://doi.org/10.1073/pnas.2106022118

alterations in the septa (Fig. 2 *E* and *F*). Pulse-chase PG labeling and superresolution fluorescence microscopy showed that the addition of either antibiotic prevents subsequent cell division (*SI Appendix*, Fig. S3*B*). Cryoelectron microscopy (cryo-EM) tomography independently confirmed the bulbous septa and plasmolysis effects of methicillin, with membrane invagination and blebs observed (*SI Appendix*, Fig. S4 and Movies S1–S5). Bulbous septa were still present when growth inhibitory concentrations of cerulenin (33) or moenomycin (34) were used in the presence of methicillin, suggesting that this phenotype is not due to continued lipid production or glycan synthesis via PBP2, respectively (*SI Appendix*, Fig. S5 *A–F*). The role of teichoic acids was determined by analysis of *tarO* and *ltaS* mutants that are missing wall teichoic or lipoteichoic acids, respectively (35, 36). The loss of either of these polymers did not reduce the plasmolysis phenotype after methicillin treatment (*SI Appendix*, Fig. S5 *G–L*). In both mutants the plasmolysis was methicillin specific, as it was not seen in the presence of vancomycin or when cells were treated with both antibiotics (*SI Appendix*, Fig. S5 *G–L*). We suggest that the plasmolysis occurs because of lesions in the cell wall that allow an explosive release of turgor, the release of cell contents, and the pulling away of the membrane from the cell wall. In the presence of methicillin, PGH activity leads to a presumptive cell scission without the synthesis of a complete septum. This in turn leads to loss of turgor around the cell emanating from this point of weakness. The observed effects were not methicillin specific, as treatment with oxacillin also resulted in cell death, volume increase, and bulbous septa, nor strain specific, as NewHG (37) treated with vancomycin or methicillin and COL (38) with vancomycin gave the same responses as SH1000 (*SI Appendix*, Fig. S6). Thus, β-lactams and vancomycin have different effects on cell morphology, suggesting that they might elicit alternative bactericidal mechanisms.

Effect of Cell Wall Antibiotics on PG Architecture. The model (Fig. 1*A*) predicts that it is continued PGH activity that leads to cell death in the presence of antibiotics, but what changes in the cell wall (e.g., general thinning, catastrophic failure etc.) is unclear. We utilized our recently developed AFM approach (28) to explore this further (Fig. 3 *A* and *B*). During the first 60 min after the addition of antibiotics, there was only a small reduction in thickness of the cell walls suggesting that overall lysis has not occurred (control = 21.19 nm, methicillin = 14.71 nm, and vancomycin = 16.04 nm) (Fig. 3*B*; $P = 5.5 \times 10^{-6}$ [methicillin] and $P = 3.4 \times 10^{-4}$ [vancomycin]). However, this was accompanied by dramatic changes to PG architecture at its inner surface (Fig. 3*A*). In contrast to healthy cells, which have a continuous fine mesh architecture characterized by a pore size of less than 10 nm (28), we observed the appearance of a significant number of holes in the fine mesh of the PG that penetrated the entire cell wall thickness (Fig. 3 *A* and *C–E* and *SI Appendix*, Fig. S7; $P = 4.3 \times 10^{-3}$ [methicillin] and $P = 1.5 \times 10^{-3}$ [vancomycin]), which are inconsistent with maintenance of turgor (28). The mesh architecture surrounding the holes appeared identical to that in untreated cells (see black and white arrows in Fig. 3*A*), implying that the holes are nucleated, via PGH activity, within the existing PG mesh architecture. After 120 min, cells are dying likely through the combination of perforating holes and reduced cell wall thickness (*SI Appendix*, Fig. S7 *G* and *H*). The effect of β-lactams was corroborated by treating the cells with oxacillin (*SI Appendix*, Fig. S7*I*). It appears that PGH activity without synthesis leads to the formation of a large number of wall-spanning holes which compromise cell viability.

To test if the action of cell wall antibiotics leads to changes in PG architecture in other species, we studied the rod-shaped, gram-positive bacterium *Bacillus subtilis*. *B. subtilis* has multiple

PGHs (39) and a PG architecture similar to that in *S. aureus*, exhibiting a tight mesh at the inside of the wall with the outside having large deep pores (28). Here, methicillin led to rapid death but without an increase in cell volume (*SI Appendix*, Fig. S8). Within 30 min, significant changes to *B. subtilis* PG architecture had occurred, with a large number of wall-spanning holes appearing at the inside surface of the wall as in *S. aureus* (*SI Appendix*, Fig. S8), establishing a likely common overarching mechanism for the action of cell wall antibiotics.

To further explore the model outlined in Fig. 1*A*, we looked for an alternative approach for interfering with PGH activity. Recently, a novel antibiotic, complestatin, has been described that binds to the cell wall and inhibits PGHs (40). While the addition of complestatin alone had some bactericidal activity, its coadministration with methicillin or vancomycin led to a significant reduction in bacterial killing by those antibiotics (Fig. 2*G* and *SI Appendix*, Fig. S9*A*). Thus, the loss of the PG synthesis leading to cell death, by the action of cell wall antibiotics, can be commuted to stasis via the inhibition of PGH, in agreement with the model (Fig. 1*A*).

Differential Antibiotic Action Reveals Two Modes of Bactericidal Activity. Methicillin and vancomycin both kill *S. aureus*, associated with a cell volume increase and the appearance of wall-spanning holes in the PG. However, methicillin alone leads to plasmolysis and a reduction in cells with complete or incomplete septa. Vancomycin treatment stops cell cycle progression as soon as it is added. Simultaneous addition of vancomycin and methicillin (or oxacillin) led to an outcome identical to vancomycin alone (Fig. 2 *A* and *F* and *SI Appendix*, Figs. S5 and S6). Also, vancomycin inhibits Triton X-100–induced cell lysis in the presence or absence of methicillin (*SI Appendix*, Fig. S9*B*). This suggested an underlying, common bactericidal mechanism between the antibiotics overlayed by another methicillin-dependent process that is inhibited by vancomycin. This second killing mode may require PGHs that are also involved in Triton X-100–induced cell lysis. Vancomycin directly inhibits the activity of Atl, the major PGH, which is also involved in lysis and septal scission (23, 41, 42). The loss of Atl led to a reduction in the rate of killing by methicillin but not vancomycin, with the methicillin-associated appearance of plasmolysis, cell swelling, and the loss of cells with complete and incomplete septa (Fig. 4 *A* and *B* and *SI Appendix*, Fig. S9 *C–E*). After 60 min of methicillin treatment, the cell wall of *atl* was thicker than SH1000 (*SI Appendix*, Fig. S7*J*). Also, in the *atl* mutant, wall-spanning holes appeared with greatly reduced area, although at the same frequency in the presence of methicillin compared to its parent (Fig. 4 *C–E*).

Vancomycin treatment leads to wall-spanning holes appearing within the fine mesh at the inside of the sacculus, where those PGHs with membrane-spanning tethers are situated. SagB is a major glucosaminidase, membrane anchored, with a pleiotropic role in physiology and growth (20, 21). A *sagB* mutation resulted in an increase of survival after vancomycin but not methicillin treatment compared to SH1000 (Fig. 4*A* and *SI Appendix*, Fig. S9*F*), although there was a reduction in cell swelling in the presence of methicillin when compared to the wild type (Fig. 4*B*). This rules out simple cell expansion and bursting as the bactericidal mechanism. After 60 min treatment with either methicillin or vancomycin, the isolated cell wall of *sagB* was thicker than the wild type (*SI Appendix*, Fig. S7*J*; $P = 0.0016$ and $P = 0.0003$, respectively). Treated with methicillin, the *sagB* mutant developed the same number and area of wall-spanning holes as SH1000, while vancomycin resulted in both fewer and smaller holes (Fig. 4 *C–E*; $P = 1.24 \times 10^{-2}$). These results demonstrate two modes of cell death associated with growth and division that, respectively, involve the major PGHs, SagB, and Atl.
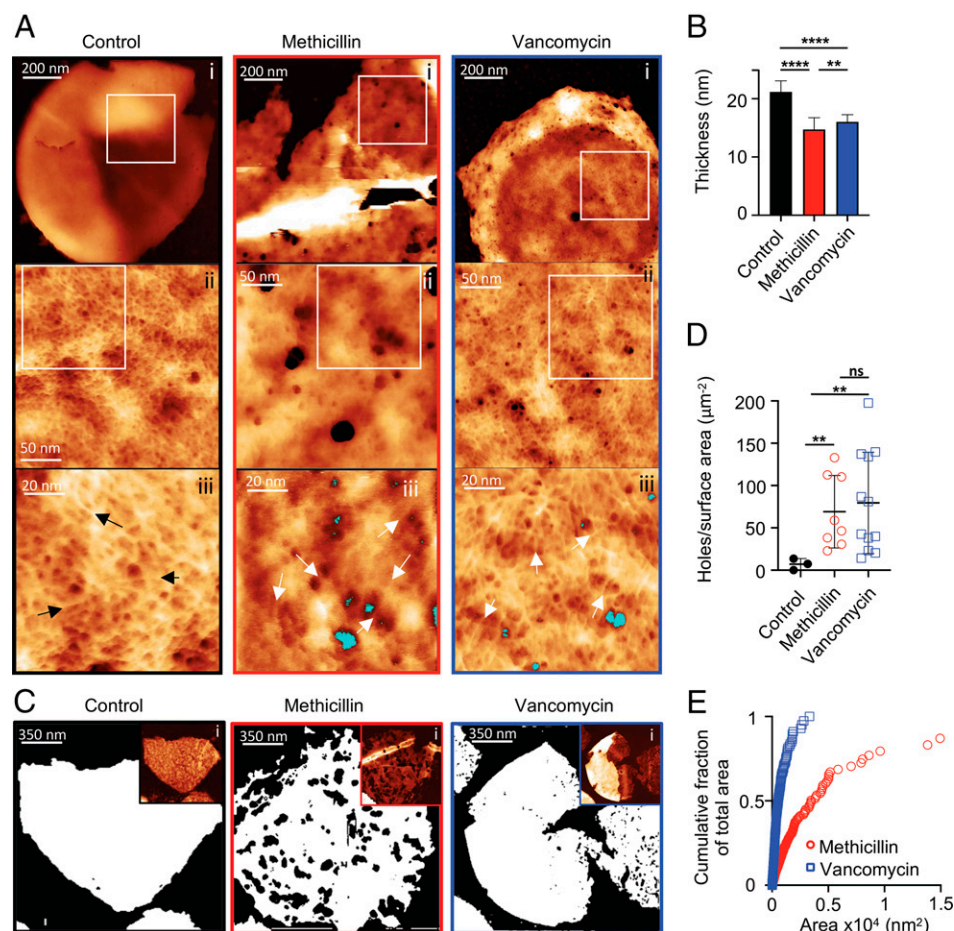
Fig. 3. The effect of cell wall antibiotics on PG architecture. (*A*) AFM images of the internal surface of isolated sacculi after 60 min treatment of cells with antibiotics. From left to right columns, black panels are the control (SH1000), red panels are methicillin-treated SH1000, and blue panels are vancomycin-treated SH1000. (*i*) In all of the columns, height channel of individual sacculi with the internal surface facing upwards, data scales (DS) = 202, 82, and 24 nm. In control, the zoomed image from the squared white area marked in *i* (*ii*), showing the internal coarse architecture displaying a smooth surface, DS = 13 nm; in methicillin and vancomycin, internal coarse architecture displaying a surface perforated by some holes that span all the way on the cell wall (*ii*), DS = 41 and 15 nm. In control, the zoomed image from the squared white area marked in *ii* (*iii*), showing the finer internal architecture, which consists of a randomly oriented glycan fibrous mesh (see black arrows) with small pores between the fibers, DS = 12 nm; in methicillin and vancomycin, randomly oriented glycan fibrous mesh (see white arrows) with small pores between the fibers next to some of the perforating holes (marked in blue) (*iii*), DS = 10 and 16 nm. (*B*) The mean height of individual sacculi in air measured by AFM after 60 min treatment of antibiotics; error bars show SD; for all samples, $n = 28$. After t test, P (control − methicillin, ****) $= 2.364 \times 10^{-17}$, P (control − vancomycin, ****) $= 5.323 \times 10^{-17}$, and P (methicillin − vancomycin, **) $= 4.816 \times 10^{-3}$. (*C*) Binary images using the threshold technique (*SI Appendix*, Fig. S7) where white = PG, black = background, the black areas inside the white sacculi correspond to holes spanning the cell wall. (*i*) Insets are the following: AFM topography images in which the binary image analysis was performed; DS = 51, 92, and 104 nm. (*D*) Holes per surface area of sacculus (micrometer squared), sample size $n = 3$, 8, and 12 from left to right; black lines represent mean value and SD. After t test with Welch's correction: p (control − methicillin, **) $= 4.3 \times 10^{-3}$, P (control − vancomycin, **) $= 1.5 \times 10^{-3}$, and P (methicillin − vancomycin, not significant [ns]) = 0.65. (*E*) Cumulative fraction of total area plotting individual perforating holes: vancomycin, $n = 899$ and methicillin, $n = 678$. For sample size and data reproducibility, see *Materials and Methods*.

Effect of PGH Deregulation on the Bactericidal Action of Antibiotics. As the diminution of PGH activity led to a reduced bactericidal rate for cell wall antibiotics (Figs. 2*G* and 4), their deregulation was explored as a mode of enhancing killing. It has been previously established that PGH activity is negatively regulated by wall teichoic acids (WTAs), which are covalently bound to the PG. The loss of WTAs in a *tarO* mutant (43) increases cell lysis because of the deregulation of endogenous PGH activity (44, 45). Here, we found that a *tarO* mutant dies more rapidly on treatment with either methicillin or vancomycin (*SI Appendix*, Fig. S10*A*), consistent with deregulated PGH activity. In fact, no viable *tarO* cells were detectable after 12 and 24 h exposure (>10^7-fold colony-forming unit [CFU] reduction, methicillin, or vancomycin, respectively), thereby removing persisters that can clinically lead to the breakdown of

antibiotic treatment regimes (46). WTA levels can be reduced by the addition of synthesis inhibitors such as tarocin A1, which also resensitizes methicillin-resistant *S. aureus* strains to β-lactams (47–49). To test if tarocin can increase the killing activity of methicillin in vivo, independent of effects on antibiotic resistance, these compounds were coadministered using the established murine sepsis model of infection with *S. aureus* NewHG (a methicillin-sensitive strain) (*SI Appendix*, Fig. S10 *B–D*). Indeed, tarocin had no effect on disease in this model, but its addition increased methicillin efficacy, with a significant reduction in the bacterial burden in the liver (*SI Appendix*, Fig. S10*D*). Thus, tarocin, as an adjunct therapy, increases methicillin effectiveness, potentially reducing the length of treatment for both antibiotic-resistant and sensitive strains.
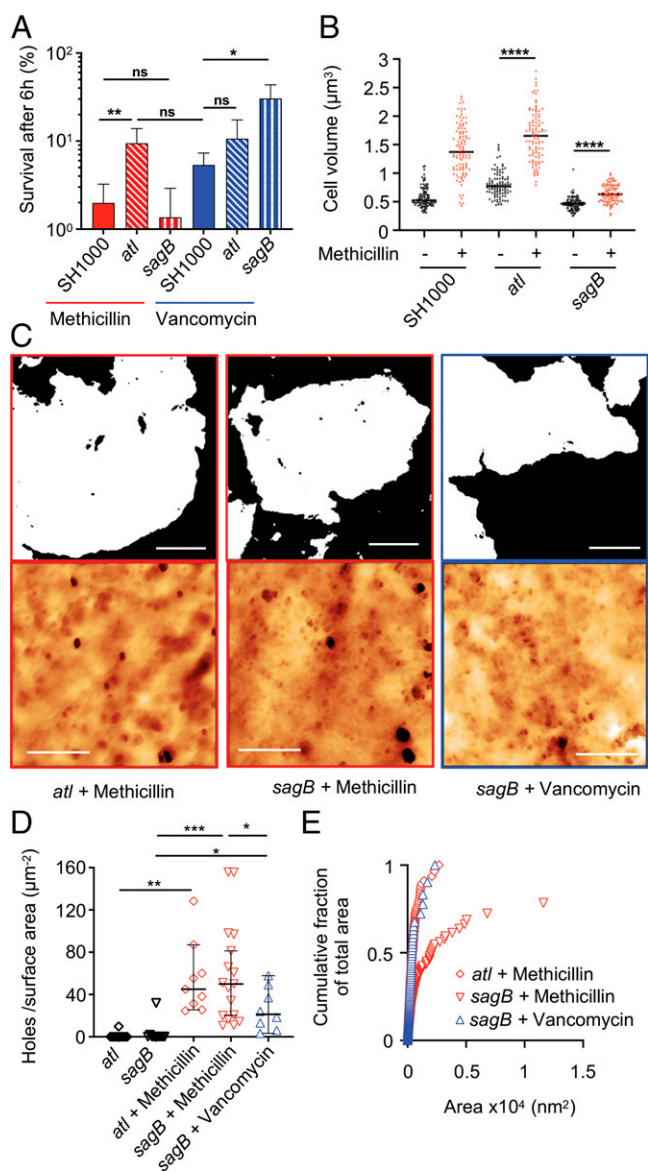
Salamaga et al.
Demonstration of the role of cell wall homeostasis in *Staphylococcus aureus* growth and the action of bactericidal antibiotics

PNAS | 5 of 8
https://doi.org/10.1073/pnas.2106022118

MICROBIOLOGY

Fig. 4. Differential role of PGH in the action of cell wall antibiotics. (*A*) Deletion of *atl* and *sagB* increases *S. aureus* survival in the presence of specific antibiotics, 6 h treatment. After *t* test with Welch's correction, P (SH1000 + methicilin − *atl* + methicillin, **) = 7.7×10^{-3}, P (SH1000 + methicillin − *sagB* + methicillin, ns) = 0.1930, P (*atl* + methicilin − SH1000 + vancomycin, ns) = 0.0737, P (SH1000 + vancomycin − *atl* + vancomycin, ns) = 0.1158, and P (SH1000 + vancomycin − *sagB* + vancomycin, *) = 0.0158. (*B*) Effect of methicillin treatment (60 min) on cell volume as measured by SIM after NHS-ester AlexaFluor 555 labeling. After *t* test with Welch's correction, P (*atl* − *atl* + methicillin, ****) = 2.305×10^{-37}, and P (*sagB* − *sagB* + methicillin, ****) = 7.685×10^{-17}. (*C*) AFM images of purified sacculi are the following: top row, binary threshold where white = PG, black = background (scale bars, 250 nm); bottom row, height channel of internal sacculus architecture of *sagB* and *atl* mutants after 10 × MIC methicillin or vancomycin treatment for 60 min (scale bars, 100 nm), data scale (DS) from left to right = 40, 40, and 30 nm. (*D*) Holes per surface area (micrometer squared), sample size n = 8, 12, and 12 from left to right. Black lines represent mean value and bars represent SD for strains treated with antibiotics for 60 min. After *t* test with Welch's correction, P (*atl* − *atl* + methicillin, **) = 1.349×10^{-3}, P (*sagB* − *sagB* + methicillin, ***) = 1.753×10^{-4}, P (*sagB* − *sagB* + vancomycin, *) = 1.546×10^{-2}, and P (*sagB* + methicillin − *sagB* + vancomycin, *) = 2.4×10^{-2}, when compared to SH1000 strain: P (SH1000 + methicillin − *atl* + methicillin, ns) = 0.47, P (SH1000 + methicillin − *sagB* + methicillin, ns) = 0.57, and P (SH1000 + vancomycin − *sagB* + vancomycin, *) = 1.24×10^{-2}. (*E*) Cumulative fraction of total area plotting individual perforating holes: *atl*, n = 408; *sagB* + methicillin, n = 488; and *sagB* + vancomycin, n = 122.

Discussion

We have investigated bacterial growth and death due to antibiotics within the context of an overall framework of multiple components responsible for PG synthesis and hydrolysis (Fig. 1*A*). Growth requires the synthesis of new PG and its subsequent hydrolysis. Here, we have separated these two processes to establish their roles. WalKR positively regulates multiple hydrolases (26), which together permit growth during the exponential phase. The (initially counterintuitive) discovery that bactericidal antibiotics prevent death of *walKR*-depleted cells can be explained, as without WalKR, the cells have reduced PGH but continued PG synthesis, resulting in death due to thickened and aberrant cell walls coupled with an inability to divide. The concomitant inhibition of PG synthesis through the action of antibiotics results in stasis (Fig. 1*A*). This explanation for cell growth establishes a clear hypothesis for the bactericidal activity of cell wall antibiotics, in which the loss of PG synthesis in the presence of PGHs would lead to cells continuing growth-associated processing of PG until it can no longer support turgor (*SI Appendix*, Fig. S11). The maturation of synthesized material via PGHs occurs without a cell volume increase per se, as the *sagB* mutant did not increase greatly in volume but died, with holes appearing at the inside surface of the cell wall.

Multiple PGHs with collective, essential roles in bacterial growth and the bactericidal activity of antibiotics underline the difficulties in identifying molecular mechanisms. This is compounded by the different effects of methicillin and vancomycin (*SI Appendix*, Fig. S11). In the presence of methicillin, those PGHs involved in cell separation, including Atl, can cleave incomplete septa, resulting in catastrophic failure, plasmolysis, and cell death. However, vancomycin inhibits some PGH activity, including Atl, preventing early septal scission and the plasmolysis observed with methicillin (*SI Appendix*, Fig. S11). Both antibiotics kill *S. aureus* with the appearance of cell wall–perforating holes, which involves the membrane-anchored PGH, SagB. The model of cell wall antibiotic action is further supported by the effect of complestatin, which, while showing some bactericidal activity itself, significantly reduces the bactericidal activity of both methicillin and vancomycin by inhibiting PGH in the absence of PG synthesis. This provides the final permutation of the original model where loss of PG synthesis or hydrolysis alone is lethal, but both is not (Fig. 1*A*). Here, we have demonstrated a simple framework for understanding both bacterial growth and the action of antibiotics in *S. aureus*, providing avenues for the development of control regimes for important antimicrobial-resistant pathogens.

Materials and Methods

Bacterial Growth Conditions. Strains used in this study are listed in *SI Appendix*, Table S1. Plasmids and oligonucleotides are listed in *SI Appendix*, Tables S2 and S3, respectively. The construction of strains used in this study are detailed in *SI Appendix*. All *S. aureus* strains were grown in tryptic soy broth (TSB), *Escherichia coli* strains in lysogeny broth, and *B. subtilis* in nutrient broth unless otherwise indicated, with appropriate antibiotics at 37 °C with agitation. For solid media 1.5% weight/volume agar was added. Plasmids were cloned using *E. coli* NEB-5α following previously described methods (50) and directly electroporated into electrocompetent *S. aureus* RN4220. The transformation and phage transduction of *S. aureus* were carried out as described previously (51, 52). Antibiotics were used at the following concentrations: vancomycin (40 µg · mL⁻¹), methicillin (40 µg · mL⁻¹), oxacillin (10 µg · mL⁻¹), cerulenin (100 µg · mL⁻¹), moenomycin (2 µg · mL⁻¹), complestatin (100 µg · mL⁻¹), erythromycin (5 µg · mL⁻¹ for SH1000; 10 µg · mL⁻¹ for LAC*), tetracycline (5 µg · mL⁻¹ for SH1000; 10 µg · mL⁻¹ for LAC*), kanamycin (50 µg · mL⁻¹ for SH1000; 90 µg · mL⁻¹ for LAC*), spectinomycin (100 µg · mL⁻¹), and ampicillin (100 µg · mL⁻¹). Complestatin was produced as previously described (40). Strains with genes under the control of the P_spac promoter were grown in the presence of IPTG at 10 µM or 1 mM as specified. azido D-alanine (ADA) and azido-D-alanyl-D-alanine;

dipeptide (ADA-DA) were produced as previously described and used at 500 µM or 1 mM concentrations, respectively (53).

Antibiotic Activity Assays. *S. aureus* strains, apart from those containing P*spac*-*walKR*, were grown overnight in TSB. The overnight cultures were used to inoculate fresh TSB media to an optical density at 600nm (OD$_{600}$) of ~0.05 and grown to an OD$_{600}$ of 0.2 to 0.3. At this point, antibiotics were added, and the change of bacterial count in the cultures was monitored. The CFU measures were normalized to the initial CFUs at the time of the antibiotic intervention, time 0.

$$\text{Survival}_{t_n}(\%) = \frac{\text{CFU}_{t_0}}{\text{CFU}_{t_n}} \cdot 100\%.$$

S. aureus P*spac*-*walKR* strains were grown in TSB supplemented with tetracycline and 1 mM IPTG overnight. Next, cells were washed in TSB and resuspended in fresh TSB supplemented with tetracycline and 10 µM IPTG to an initial OD$_{600}$ of 0.1. The cultures were grown to an OD$_{600}$ of 0.5 and washed three times in TSB. Cells were resuspended in fresh TSB supplemented with tetracycline and incubated either with 1 mM IPTG (WalKR ON) or without IPTG (WalKR OFF) in the presence or absence of cell wall antibiotics. The change of bacterial count in the cultures was monitored. The CFU measures were normalized to the initial CFUs at the time of the antibiotic intervention, time 0.

$$\text{Relative CFU} = \frac{\text{CFU}_{t_0}}{\text{CFU}_{t_n}} \cdot 100\%.$$

There were at least three biological replicates of each assay.

Triton X-100–Induced Lysis. *S. aureus* strains were grown to midlog phase (OD$_{600}$ ~0.4), washed by centrifugation, and resuspended in 0.1% volume/volume Triton X-100 in phosphate-buffered saline to a final OD$_{600}$ of ~0.8, with or without addition of antibiotics. Cell lysis was monitored by OD$_{600}$ measurements.

Purification of PG Sacculi. PG was purified as described previously (54), although some alterations were performed. Briefly, 1 L bacterial culture was grown to an OD$_{600}$ of 0.2 to 0.3 and then antibiotics were added as required. A minimum of 200 mL of culture was used at each time point (e.g., 60 min). Cell suspensions were boiled (10 min) and cells harvested by centrifugation (5,000 *g*, 5 min, room temperature [RT]). The cells were mechanically broken and sacculi purified (54).

Radioactive ^{14}C-GlcNAc Incorporation. *S. aureus* strains were grown, and 1 mL of cell culture was added to 2.5 µL of ^{14}C-GlcNAc for a final concentration of 5 µM ^{14}C-GlcNAc. The sample was incubated shaking at 37 °C for 5 min, collected, and prepared for analysis of ^{14}C-GlcNAc incorporation via Liquid Scintillation as previously described (55).

ADA or ADA-DA Labeling of PG. *S. aureus* cells were incubated with ADA or dipeptide [produced as previously described (53)] on a rotary shaker at 37 °C for 5 min. Cells were then fixed and labeled by Click chemistry. Dipeptide containing an azide functional group required chemical attachment of a fluorophore via the Click reaction (copper [I]-catalyzed alkyne-azide cycloaddition). This was carried out using the Click-iT Cell Reaction Buffer Kit (Thermo Fisher) as per the manufacturer's protocol. Alkyne dyes were added at 5 µg/mL.

Microscopy Approaches. The study used a combination of fluorescence, atomic force, transmission electron, and cryo-EM approaches throughout. Methods and analyses and detailed in *SI Appendix*.

Ethics Statement. Animal work was completed in accordance with UK law in the Animals (Scientific Procedures) Act 1986 under Project License P3BFD6DB9 for murine experiments with approval of the Sheffield Ethical Review Committee.

Murine Sepsis Infection. In all experiments, 6 to 8-wk-old female BALB/c mice (Charles River Laboratories) were used. Mice were housed in designated animal facilities following standard husbandry protocols at the University of Sheffield. Bacteria were prepared for murine injection (56), in which 100 µL of *S. aureus* (1 × 10^7 CFU/mL) was injected intravenously into the tail vein of each mouse, with 10 mice in each experimental group. Mice were monitored daily (health and weight) and were euthanized at the experimental end point. Organ CFU at the experimental endpoint was calculated (57) for livers and kidneys. For the analysis of methicillin and tarocin A1 in the murine sepsis model, the NewHG (kan^R) *S. aureus* strain was injected. At 21 and 25 hpi, mice were subcutaneously injected with 100 µL containing either 1 mg tarocin A1 (SML1677-25MG, Sigma-Aldrich), 2.5 mg methicillin (51454-50mg, Sigma-Aldrich), both tarocin A1 and methicillin, or a vehicle control, and mice were euthanized at 48 h after infection.

1. A. L. Koch, Growth and form of the bacterial cell wall. *Am. Sci.* **78**, 327–341 (1990).
2. A. K. Yadav, A. Espaillat, F. Cava, Bacterial strategies to preserve cell wall integrity against environmental threats. *Front. Microbiol.* **9**, 2064 (2018).
3. T. Dörr, P. J. Moynihan, C. Mayer, Editorial: Bacterial cell wall structure and dynamics. *Front. Microbiol.* **10**, 2051 (2019).
4. R. D. Turner, W. Vollmer, S. J. Foster, Different walls for rods and balls: The diversity of peptidoglycan. *Mol. Microbiol.* **91**, 862–874 (2014).
5. W. Vollmer, D. Blanot, M. A. de Pedro, Peptidoglycan structure and architecture. *FEMS Microbiol. Rev.* **32**, 149–167 (2008).
6. T. Schneider, H. G. Sahl, An oldie but a goodie—Cell wall biosynthesis as antibiotic target pathway. *Int. J. Med. Microbiol.* **300**, 161–169 (2010).
7. H. Cho, T. Uehara, T. G. Bernhardt, Beta-lactam antibiotics induce a lethal malfunctioning of the bacterial cell wall synthesis machinery. *Cell* **159**, 1300–1311 (2014).
8. P. Giesbrecht, T. Kersten, H. Maidhof, J. Wecke, Staphylococcal cell wall: Morphogenesis and fatal variations in the presence of penicillin. *Microbiol. Mol. Biol. Rev.* **62**, 1371–1414 (1998).
9. Y. Kawai *et al.*, Crucial role for central carbon metabolism in the bacterial L-form switch and killing by β-lactam antibiotics. *Nat. Microbiol.* **4**, 1716–1726 (2019).
10. M. A. Kohanski, D. J. Dwyer, B. Hayete, C. A. Lawrence, J. J. Collins, A common mechanism of cellular death induced by bactericidal antibiotics. *Cell* **130**, 797–810 (2007).
11. A. Tomasz, The mechanism of the irreversible antimicrobial effects of penicillins: How the beta-lactam antibiotics kill and lyse bacteria. *Annu. Rev. Microbiol.* **33**, 113–137 (1979).
12. A. Tomasz, A. Albino, E. Zanati, Multiple antibiotic resistance in a bacterium with suppressed autolytic system. *Nature* **227**, 138–140 (1970).
13. T. K. Lee, K. C. Huang, The role of hydrolases in bacterial cell-wall growth. *Curr. Opin. Microbiol.* **16**, 760–766 (2013).
14. W. Vollmer, B. Joris, P. Charlier, S. Foster, Bacterial peptidoglycan (murein) hydrolases. *FEMS Microbiol. Rev.* **32**, 259–286 (2008).
15. C. Goffin, J. M. Ghuysen, Multimodular penicillin-binding proteins: An enigmatic family of orthologs and paralogs. *Microbiol. Mol. Biol. Rev.* **62**, 1079–1093 (1998).
16. A. Wada, H. Watanabe, Penicillin-binding protein 1 of *Staphylococcus aureus* is essential for growth. *J. Bacteriol.* **180**, 2759–2765 (1998).
17. S. F. Pereira, A. O. Henriques, M. G. Pinho, H. de Lencastre, A. Tomasz, Role of PBP1 in cell division of *Staphylococcus aureus*. *J. Bacteriol.* **189**, 3525–3531 (2007).
18. S. F. Pereira, A. O. Henriques, M. G. Pinho, H. de Lencastre, A. Tomasz, Evidence for a dual role of PBP1 in the cell division and cell separation of *Staphylococcus aureus*. *Mol. Microbiol.* **72**, 895–904 (2009).
19. M. G. Pinho, S. R. Filipe, H. de Lencastre, A. Tomasz, Complementation of the essential peptidoglycan transpeptidase function of penicillin-binding protein 2 (PBP2) by the drug resistance protein PBP2A in *Staphylococcus aureus*. *J. Bacteriol.* **183**, 6525–6531 (2001).
20. R. Wheeler *et al.*, Bacterial cell enlargement requires control of cell wall stiffness mediated by peptidoglycan hydrolases. *MBio* **6**, e00660 (2015).
21. Y. G. Chan, M. B. Frankel, D. Missiakas, O. Schneewind, SagB glucosaminidase is a determinant of *staphylococcus aureus* glycan chain length, antibiotic susceptibility, and protein secretion. *J. Bacteriol.* **198**, 1123–1136 (2016).
22. S. J. Foster, Molecular characterization and functional analysis of the major autolysin of *Staphylococcus aureus* 8325/4. *J. Bacteriol.* **177**, 5723–5725 (1995).
23. T. Oshida *et al.*, A *Staphylococcus aureus* autolysin that has an N-acetylmuramoyl-L-alanine amidase domain and an endo-beta-N-acetylglucosaminidase domain: Cloning, sequence analysis, and characterization. *Proc. Natl. Acad. Sci. U.S.A.* **92**, 285–289 (1995).

Salamaga et al.
Demonstration of the role of cell wall homeostasis in *Staphylococcus aureus* growth and the action of bactericidal antibiotics

PNAS | 7 of 8
https://doi.org/10.1073/pnas.2106022118

MICROBIOLOGY

24. J. Kajimura *et al.*, Identification and molecular characterization of an N-acetylmuramyl-L-alanine amidase Sle1 involved in cell separation of *Staphylococcus aureus*. *Mol. Microbiol.* **58**, 1087–1101 (2005).

25. A. Delauné *et al.*, The WalKR system controls major staphylococcal virulence genes and is involved in triggering the host inflammatory response. *Infect. Immun.* **80**, 3438–3453 (2012).

26. A. Delaune *et al.*, Peptidoglycan crosslinking relaxation plays an important role in *Staphylococcus aureus* WalKR-dependent cell viability. *PLoS One* **6**, e17054 (2011).

27. S. Dubrac, P. Bisicchia, K. M. Devine, T. Msadek, A matter of life and death: Cell wall homeostasis and the WalKR (YycGF) essential signal transduction pathway. *Mol. Microbiol.* **70**, 1307–1322 (2008).

28. L. Pasquina-Lemonche *et al.*, The architecture of the Gram-positive bacterial cell wall. *Nature* **582**, 294–297 (2020).

29. M. B. Frankel, A. P. Hendrickx, D. M. Missiakas, O. Schneewind, LytN, a murein hydrolase in the cross-wall compartment of *Staphylococcus aureus*, is involved in proper bacterial growth and envelope assembly. *J. Biol. Chem.* **286**, 32593–32605 (2011).

30. M. R. Stapleton *et al.*, Characterization of IsaA and SceD, two putative lytic transglycosylases of *Staphylococcus aureus*. *J. Bacteriol.* **189**, 7316–7325 (2007).

31. L. Zheng, M. Yan, F. Fan, Y. Ji, The essential WalK histidine kinase and WalR regulator differentially mediate autolysis of *Staphylococcus aureus* RN4220. *J. Nat. Sci.* **1**, e111 (2015).

32. S. Dubrac, T. Msadek, Identification of genes controlled by the essential YycG/YycF two-component system of *Staphylococcus aureus*. *J. Bacteriol.* **186**, 1175–1181 (2004).

33. R. P. Adhikari, R. P. Novick, Subinhibitory cerulenin inhibits staphylococcal exoprotein production by blocking transcription rather than by blocking secretion. *Microbiology (Reading)* **151**, 3059–3069 (2005).

34. Y. Rebets *et al.*, Moenomycin resistance mutations in *Staphylococcus aureus* reduce peptidoglycan chain length and cause aberrant cell division. *ACS Chem. Biol.* **9**, 459–467 (2014).

35. C. Weidenmaier *et al.*, Lack of wall teichoic acids in *Staphylococcus aureus* leads to reduced interactions with endothelial cells and to attenuated virulence in a rabbit model of endocarditis. *J. Infect. Dis.* **191**, 1771–1777 (2005).

36. R. M. Corrigan, J. C. Abbott, H. Burhenne, V. Kaever, A. Gründling, c-di-AMP is a new second messenger in *Staphylococcus aureus* with a role in controlling cell size and envelope stress. *PLoS Pathog.* **7**, e1002217 (2011).

37. E. S. Duthie, L. L. Lorenz, Staphylococcal coagulase; mode of action and antigenicity. *J. Gen. Microbiol.* **6**, 95–107 (1952).

38. W. M. Shafer, J. J. Iandolo, Genetics of staphylococcal enterotoxin B in methicillin-resistant isolates of *Staphylococcus aureus*. *Infect. Immun.* **25**, 902–911 (1979).

39. T. J. Smith, S. A. Blackman, S. J. Foster, Autolysins of *Bacillus subtilis*: Multiple enzymes with multiple functions. *Microbiology (Reading)* **146**, 249–262 (2000).

40. E. J. Culp *et al.*, Evolution-guided discovery of antibiotics that inhibit peptidoglycan remodelling. *Nature* **578**, 582–587 (2020).

41. R. Biswas *et al.*, Activity of the major staphylococcal autolysin Atl. *FEMS Microbiol. Lett.* **259**, 260–268 (2006).

42. J. Eirich, R. Orth, S. A. Sieber, Unraveling the protein targets of vancomycin in living *S. aureus* and *E. faecalis* cells. *J. Am. Chem. Soc.* **133**, 12144–12153 (2011).

43. C. Weidenmaier *et al.*, Role of teichoic acids in *Staphylococcus aureus* nasal colonization, a major risk factor in nosocomial infections. *Nat. Med.* **10**, 243–245 (2004).

44. M. Schlag *et al.*, Role of staphylococcal wall teichoic acid in targeting the major autolysin Atl. *Mol. Microbiol.* **75**, 864–873 (2010).

45. R. Biswas *et al.*, Proton-binding capacity of *Staphylococcus aureus* wall teichoic acid and its role in controlling autolysin activity. *PLoS One* **7**, e41415 (2012).

46. B. Gollan, G. Grabe, C. Michaux, S. Helaine, Bacterial persisters and infection: Past, present, and progressing. *Annu. Rev. Microbiol.* **73**, 359–385 (2019).

47. J. Campbell *et al.*, Synthetic lethal compound combinations reveal a fundamental connection between wall teichoic acid and peptidoglycan biosyntheses in *Staphylococcus aureus*. *ACS Chem. Biol.* **6**, 106–116 (2011).

48. M. A. Farha *et al.*, Inhibition of WTA synthesis blocks the cooperative action of PBPs and sensitizes MRSA to β-lactams. *ACS Chem. Biol.* **8**, 226–233 (2013).

49. S. H. Lee *et al.*, TarO-specific inhibitors of wall teichoic acid biosynthesis restore β-lactam efficacy against methicillin-resistant staphylococci. *Sci. Transl. Med.* **8**, 329ra32 (2016).

50. J. Sambrook, E. F. Fritsch, T. Maniatis, *Molecular Cloning: A Laboratory Manual* (Cold Spring Harbor Laboratory Press, Cold Spring Harbor, NY, 1989).

51. R. P. Novick, S. I. Morse, In vivo transmission of drug resistance factors between strains of *Staphylococcus aureus*. *J. Exp. Med.* **125**, 45–59 (1967).

52. S. Schenk, R. A. Laddaga, Improved method for electroporation of *Staphylococcus aureus*. *FEMS Microbiol. Lett.* **73**, 133–138 (1992).

53. V. A. Lund *et al.*, Molecular coordination of *Staphylococcus aureus* cell division. *eLife* **7**, e32057 (2018).

54. R. D. Turner, J. K. Hobbs, S. J. Foster, Atomic force microscopy analysis of bacterial cell wall peptidoglycan architecture. *Methods Mol. Biol.* **1440**, 3–9 (2016).

55. H. Maki, K. Miura, Y. Yamano, Katanosin B and plusbacin A(3), inhibitors of peptidoglycan synthesis in methicillin-resistant *Staphylococcus aureus*. *Antimicrob. Agents Chemother.* **45**, 1823–1827 (2001).

56. V. V. Panchal *et al.*, Evolving MRSA: High-level β-lactam resistance in *Staphylococcus aureus* is associated with RNA Polymerase alterations and fine tuning of gene expression. *PLoS Pathog.* **16**, e1008672 (2020).

57. E. Boldock *et al.*, Human skin commensals augment *Staphylococcus aureus* pathogenesis. *Nat. Microbiol.* **3**, 881–890 (2018).

8 of 8 | **PNAS**
https://doi.org/10.1073/pnas.2106022118

Salamaga et al.
Demonstration of the role of cell wall homeostasis in *Staphylococcus aureus* growth and the action of bactericidal antibiotics